

Are moving punctures equivalent to moving black holes?

**Jonathan Thornburg^{1,2}, Peter Diener^{3,4}, Denis Pollney^{1,3},
Luciano Rezzolla^{1,4}, Erik Schnetter^{3,4}, Ed Seidel^{3,4}, Ryoji Takahashi^{3,5}**

¹ Max-Planck-Institut für Gravitationsphysik, Albert-Einstein-Institut, Potsdam, Germany

² School of Mathematics, University of Southampton, Southampton, England

³ Center for Computation & Technology, Louisiana State University, Baton Rouge, LA, USA

⁴ Department of Physics and Astronomy, Louisiana State University, Baton Rouge, LA, USA

⁵ Instituto de Ciencias Nucleares, Universidad Nacional Autónoma de México, México D.F., México

Abstract. When simulating the inspiral and coalescence of a binary black-hole system, special care needs to be taken in handling the singularities. Two main techniques are used in numerical-relativity simulations: A first and more traditional one “excises” a spatial neighbourhood of the singularity from the numerical grid on each spacelike hypersurface. A second and more recent one, instead, begins with a “puncture” solution and then evolves the full 3-metric, including the singular point. In the continuum limit, excision is justified by the light-cone structure of the Einstein equations and, in practice, can give accurate numerical solutions when suitable discretizations are used. However, because the field variables are non-differentiable at the puncture, there is no proof that the moving-punctures technique is correct, particularly in the discrete case. To investigate this question we use both techniques to evolve a binary system of equal-mass non-spinning black holes. We compare the evolution of two curvature 4-scalars with proper time along the invariantly-defined worldline midway between the two black holes, using Richardson extrapolation to reduce the influence of finite-difference truncation errors. We find that the excision and moving-punctures evolutions produce the same invariants along that worldline, and thus the same spacetimes throughout that worldline’s causal past. This provides convincing evidence that moving-punctures are indeed equivalent to moving black holes.

PACS numbers: 04.25.Dm, 04.30.Db, 04.70.Bw, 95.30.Sf, 97.60.Lf

1. Introduction and Motivations

Binary black hole coalescences are both natural laboratories in which to study the nonlinear strong-field dynamics of General Relativity and among the most promising sources of gravitational radiation for modern laser-interferometric detectors. Despite these being very simple systems, as the black holes are assumed to be in vacuum and the solution of the Einstein equations fully describes the binary, no analytic solutions are known and numerical methods represent the only viable approach to investigate these systems’ strong-field dynamics. The past few years have seen major advances in these numerical simulations, with demonstrations of multiple orbit evolutions through merger [1, 2, 3, 4, 5], recoils from unequal-mass systems [6, 7], and studies of spin couplings in the final orbit [8, 9, 10]. Convergence

studies and cross-checks between independent codes [11] have demonstrated an impressive consistency, lending support to their credibility as reliable modellers of these sources.

Any such numerical simulation must use some means to treat the singularities contained within the black holes and modern simulations therefore use different techniques to treat the black holes, either “excision” or “moving punctures”. The excision technique [12] can use a slicing which intersects the singularity, but removes part of the interior of the horizon from the numerical domain on each slice. Excision is straightforward in spherical symmetry, but technically more difficult to implement in higher dimensions for grids using Cartesian coordinates, in which the excision region is an irregular surface of spherical topology. The simplest case is that of “stationary” excision, where once a given grid point is excised, it stays excised for the remainder of the numerical simulation. For an orbiting binary black hole system this requires using coordinates which corotate with the black holes. This technique has been used by several authors (see, *e.g.*, [13, 14, 15, 16]) but we have so far not been able to compute useful waveforms from inspiral simulations using this technique. In contrast, a technically more difficult form of excision allows the excision region to move with respect to the numerical grid. This technique has also been used by several authors (see, *e.g.*, [17, 18, 19, 1, 2, 20]) and in some cases has allowed the calculation of waveforms [1, 2, 20].

The “moving puncture” technique, on the other hand, makes use of “puncture data” [21] which are evolved *without excision* using suitable gauges [22] and allowing the singularities to be advected across the computational grid [23, 24]. We recall that by this method the curvature singularity at the centre of a black hole is avoided and replaced by an asymptotically flat spacetime through the throat. A coordinate singularity at the effective $r = 0$ of each black hole still remains, and this represents a non-differentiable point which, at least in principle, needs special treatment. Standard finite-difference techniques, in fact, require smooth functions at each gridpoint and thus would not be able to evaluate derivatives in the neighbourhood of the puncture. In practice, however, the inaccuracies at these points are isolated and, at least in the continuum limit, the physical causality of the spacetime ensures that these errors do not propagate out of the horizon. In addition, the standard singularity-avoiding gauge conditions used in puncture evolutions lead to spacetimes that are essentially stationary in their neighbourhood. This has been pointed out in [25] and more extensively discussed in [26].

An important remark should be made at this point. Mathematically, either use of the excision or moving-punctures technique is justified by the light-cone causality of the Einstein equations near a black hole, which guarantee that within the horizon physical modes only propagate inwards, towards the spacelike excision boundary or the puncture. In practice, there are two factors which complicate this picture. Firstly, the conformal-traceless formulations of the Einstein equations [27, 28, 29] evolution system, with the commonly used gauges, are known to have gauge modes which propagate superluminally in the neighbourhood of the black hole [30]. And secondly, it is only in the *continuum form* that the characteristic structure completely determines the causality. For the *discretized form* of the Einstein equations, numerical errors having high spatial frequencies with respect to the grid spacing are inevitably generated. Such signals are not propagated accurately by a finite-differencing scheme and,

in particular, they are not constrained to propagate within the light cone; indeed they can propagate at any speeds up to the finite-difference domain of dependence speed. It is thus not obvious that such spurious modes will remain confined within the black hole horizon. This concept is so essential for understanding this work that we will stress it again: there are as yet no rigorous proofs that either excision or moving-punctures techniques yield stable evolution schemes for the conformal-traceless formulations of the Einstein equations, or that if so, that the results will converge to a (correct) solution of the Einstein equations as the grid is refined.

The purpose of this paper is to improve our confidence in both methods in situations that go beyond simple static or stationary solution of isolated black holes. We do this by comparing the spacetimes generated using corotating-excision (CE) and moving-punctures (MP) evolutions of the same initial data, representing an equal-mass non-spinning binary black hole in its last orbit before coalescence. In particular, we concentrate on the evolution of two curvature invariants measured along a well-defined geodesic between the two black holes and provide the first strong-field evidence that excised and moving-puncture yield the same solution of the Einstein equations for this system.

2. Methods and Results

The simplest way to compare evolutions of binary systems using either CE or MP techniques would involve the direct use of gauge-invariant quantities such as waveforms. Indeed, this has been done in [31], for head-on collisions of pure puncture evolutions, as well as in [11], where waveforms coming from different implementations of the moving puncture technique and from a generalized harmonic formulation of the Einstein equations [2] were compared. While both of these works have shown there are close similarities in the waveforms, they have also highlighted small differences. Most importantly, however, the comparisons were not using Richardson extrapolation to reduce the influence of finite-difference truncation errors. Unfortunately, because of technical complications in the wave-extraction when using corotating coordinates, the evolutions of corotating and excised punctures have not produced usable asymptotic waveforms [14, 16] ([32] presents a possible route to overcoming these problems). Thus, the use of waveforms is not a viable route for this comparison.

However, an alternative route, which also allows to probe regions of the spacetime with strong and highly dynamical curvature, consists of first identifying corresponding events in the two spacetimes, and then gauge-transform quantities that are gauge-dependent. (Note that similar issues arise in almost any comparison of different numerical-relativity codes [33].). For an equal-mass binary system this is particularly simple and to identify corresponding events we consider the central worldline midway between the two black holes. The initial data has π -symmetry about this worldline, and this is preserved by both evolutions, so this worldline is invariantly defined. We can thus use proper time along this worldline as a 4-invariant parameterization, matching up corresponding events in the two simulations.

All the numerical simulations for both corotating excision and moving punctures have been performed using the same evolution code and initial data. The latter, in particular, are constructed as in [34] and have orbital parameters to approximate a binary system of non-

spinning black holes in quasi-circular orbit, with initial proper separation $L = 9.32M$, mass parameters $m = 0.47656M$, where M is the total mass of the system, and equal and opposite linear momenta $p = \pm 0.13808M$ [14]. The evolutions are carried out using a conformal-traceless formulation of the Einstein equations as described in [22], with “1+log” slicing and Γ -driver shift. The CE runs benefit from insights gained in [16] and use the GC2 gauge condition of that work. The MP runs use the optimal gauge conditions of [35], with the lapse evolved via $\partial_t \alpha = -2\alpha K + \beta^i \partial_i \alpha$, while the shift evolution follows prescription 8 in Table I of [35] with $\eta = 0.5$. Individual apparent horizons are located every few timesteps during the evolution [36, 37]. The code is implemented in the Cactus framework.

Spatial differentiation is performed via straightforward finite-differencing using second- or fourth-order algorithms for CE and MP, respectively. In addition, for the MP runs a fifth-order Kreiss-Oliger artificial dissipation is also added to all evolution variables. Vertex-centred AMR is employed using nested mesh-refined grids [38] with the highest resolution concentrated in the neighbourhood of the individual horizons. In the case of CE evolutions, eight levels of refinement have been used; the corotating gauge conditions guarantee that the black holes remain on the fine grids throughout the evolution. In the case of MP evolutions, on the other hand, nine levels of refinement are used, with the finest two levels being locked to the position of the centroid of the apparent horizon. For either the CE or MP approach, we have carried out simulations with at least three different resolutions. However, because the two approaches have rather different truncation errors, with MP using higher-order finite differencing, the CE simulations have fine-grid spatial resolutions of $h = 0.018, 0.015$, and $0.0125 M$, while the MP ones have coarser resolutions, with $h = 0.032, 0.025$, and $0.020 M$.

As mentioned earlier, an unambiguous measure of the CE and MP spacetimes can be made by using the 4-invariant spacetime curvature scalars $I \equiv \tilde{C}_{\alpha\beta\gamma\delta} \tilde{C}^{\alpha\beta\gamma\delta}$ and $J \equiv \tilde{C}_{\alpha\beta\gamma\delta} \tilde{C}^{\gamma\delta}_{\mu\nu} \tilde{C}^{\mu\nu\alpha\beta}$, where $\tilde{C}_{\alpha\beta\gamma\delta} = C_{\alpha\beta\gamma\delta} + \frac{1}{2}i\epsilon_{\alpha\beta\mu\nu} C^{\mu\nu}_{\gamma\delta}$ is the self-dual part of the Weyl tensor $C_{\alpha\beta\gamma\delta}$. Note that while I and J are complex numbers, for our evolutions their real parts are at least 12 orders of magnitude larger than the imaginary ones, so that $I, J = \Re(I, J)$ to very good precision. Hereafter we will concentrate on reporting results for I only, as a very similar behaviour is found also for J .

The measure of the invariants has to be made along exactly the same worldline in the two spacetimes, and when the black holes have equal masses, the spatial point midway between the black holes is invariantly defined, and its worldline can be used for this measure. Clearly, evolutions with different gauges will generate different coordinate descriptions of this point, but this ambiguity is absent when the affine parameter along the geodesic is chosen to be the proper time τ . As a result, I expressed as a function of τ along the worldline of the midway point between the two black holes can be used as a gauge-invariant diagnostic of the evolution. We note that because $I(\tau)$ has a super-exponential behaviour, all of the analysis has been performed in terms of $\log I$ to increase accuracy.

Figure 1 shows the evolution in coordinate time of $\log I$ for the MP evolutions (solid lines) and the smoothed CE ones (dashed lines). The raw I -timeseries for the CE evolutions are quite noisy (cf. small squares in Fig. 1), and for further analysis we smoothed these with a fourth-order Savitzky-Golay filter [39] over a $\pm 10 M$ sliding window in coordinate time. We

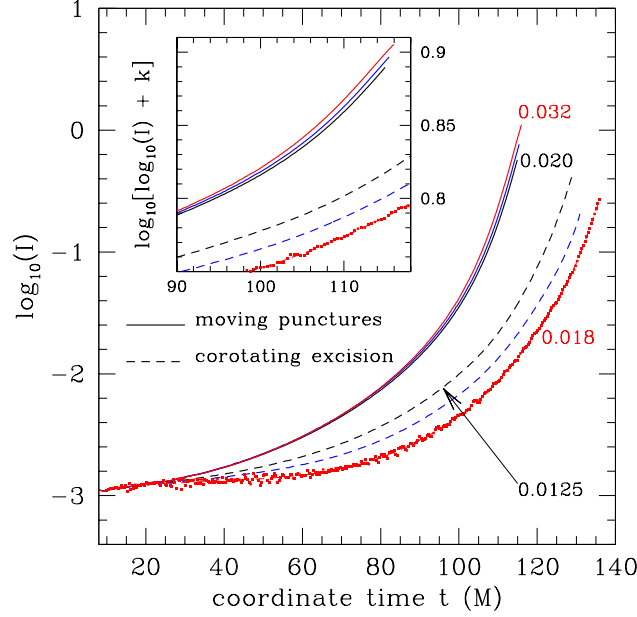


Figure 1. Evolution in coordinate time of $\log I$ for the MP evolutions (solid lines) and the smoothed CE ones (dashed lines), while the raw CE-data is indicated with squares for the coarsest resolution only. A magnification of the overlapping MP curves is shown in the inset.

have verified the smoothing does not introduce systematic errors; no smoothing was necessary for the MP evolutions.

Because it is not practical to make h small enough so that finite-differencing errors are negligible, we exploit the known convergence properties of finite-difference schemes to Richardson-extrapolate our finite- h results to the limit $h \rightarrow 0$. In particular, given some quantity u computed at numerical resolution h , we write the Richardson-extrapolation series $u(h)$ as $u(h) = u(0) + ph^n + qh^{n+1} + \mathcal{O}(h^{n+2})$, where $n=2$ (4) for CE (MP), and where the coefficients p and q depend on u , but not on the resolution h . Given $u(h)$ at three distinct resolutions, we solve for $u(0)$ as the Richardson-extrapolated value for u , i.e., $\mathcal{R}(u) \equiv u(0)$. Clearly, slightly different values for $\mathcal{R}(u)$ will be obtained depending on which of the higher-order terms are neglected in the series expansion, and we use the magnitude of the last known term in the expansion at the highest resolution as a rough estimate of the errors in $\mathcal{R}(u)$.

In practice, for each evolution we have first extracted the timeseries of α and I up to the detection of a common apparent horizon and then time-integrated $\alpha(t)$ to obtain $\tau(t)$, as shown in Fig. 2 for simulations using MP (thin solid lines) or CE (thin dashed lines). Using this data and the Richardson-extrapolation series expansion, an estimate for $\mathcal{R}(\tau(t))$ is then obtained and shown with thick lines (solid for MP and dashed for CE), with the inset offering a view. Despite having lower resolutions, the MP evolutions show a closer match between the different resolutions and the Richardson-extrapolated result than do the CE ones.

Finally, we have Richardson-extrapolated $\log I(t)$, and removed the dependence on the time coordinate by mapping t to $\mathcal{R}(\tau(t))$ (cf. Fig. 2). Our end results are therefore $\mathcal{R}(\log I_{\text{CE}})$ and $\mathcal{R}(\log I_{\text{MP}})$, both as functions of $\mathcal{R}(\tau)$.

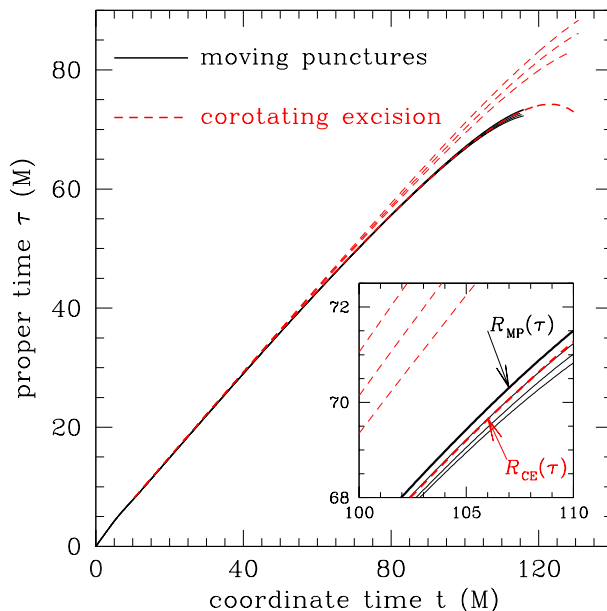


Figure 2. Relationship between coordinate time t and proper time τ for simulations using MP (solid lines) or CE (dashed lines). The inset offers a magnification over a representative window in time.

The results of this procedure are summarized in Fig. 3, which shows the proper-time evolution of $\log I(\tau)$, together with the estimated error bands. More specifically, thick lines show the Richardson-extrapolated results (solid for MP and dashed for CE) while the dotted lines report the error bars, with the larger ones referring to CE evolutions. Clearly, the two Richardson-extrapolated evolutions of the invariant lie well within the estimated error-bands for both evolutions and are almost indistinguishable for large portions of the simulations, despite the large dynamical range. The inset highlights this, with a view in a representative window in proper time. Overall, the results in Fig. 3, together with the similar ones for J , demonstrate that, despite the different gauges and the different way in which the singularities are treated in the two approaches, the two approaches are indeed converging to the same spacetime, at least along the fiducial central geodesic.

3. Conclusions

Excision and moving punctures both seem to work well in practice, and are used by multiple research groups, yet lack rigorous mathematical correctness proofs. To help improve our confidence in both methods, we have compared them by evolving the same equal-mass non-spinning binary black hole system using both corotating-excision and moving-punctures techniques. Comparing the evolution of the I and J curvature 4-scalars with proper time along the invariantly-defined worldline midway between the two black holes, and using Richardson extrapolation to reduce the effects of finite-difference truncation errors, we find that moving-punctures and excision evolutions agree to within our estimated numerical errors.

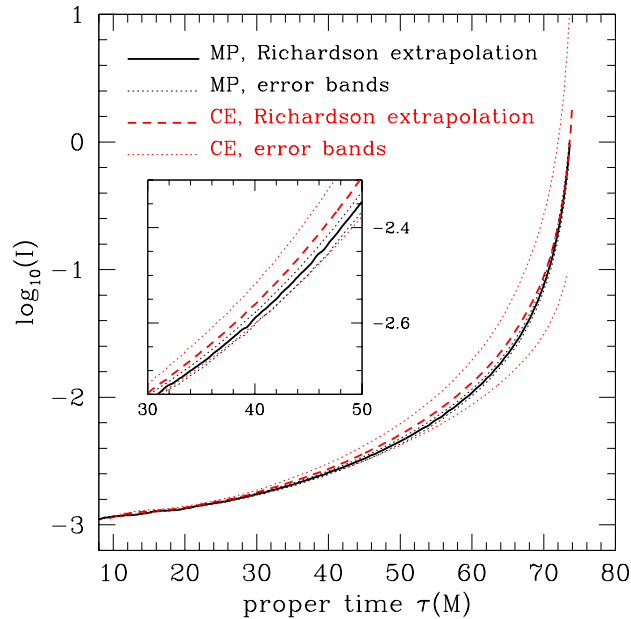


Figure 3. $\log I(\tau)$ for each evolution family, together with the estimated errors. Thick lines show the Richardson-extrapolated results (solid for MP and dashed for CE) while the dotted lines report the error bars, with the larger ones referring to CE evolutions. Note the excellent agreement as highlighted in the inset.

I and J are sensitive and nonlinear functions of many components of the Riemann tensor with markedly different nonlinearities: I is quadratic in the Riemann tensor, while J is cubic. The fact they both agree in the two different techniques makes it very unlikely that this is just an artifact of the symmetry. A rigorous proof of the equivalence of the two spacetimes would require a detailed examination of the curvature components and their derivatives in an invariant frame [40]. However, the established equivalence of I and J is a strong validation that the entire Riemann tensors for this algebraically general spacetime agree along the central worldline. Given the causal structure of the Einstein equations, this agreement extends to the entire causal past of the central worldline. Furthermore, because our data span a time much longer than the initial separation of the two black holes (our evolutions last for $\sim 70 M$, while the initial separation is $\sim 9 M$), the causal past of central worldline includes a large part of the strong-field region of the spacetime extending well out into the wave zone. Therefore, for the evolutions reported here these results provide convincing evidence that the corotating-excision and the moving-punctures techniques yield the same spacetime as solution of the Einstein equations.

Acknowledgments

The numerical calculations were performed on *Peyote* and *Belladonna* at AEI, *Jacquard* at NERSC, *Tungsten* at NCSA, *Supermike* and *Santaka* at LSU and on *Ducky* and *Neptune* at LONI. This work was supported in part by the DFG grant SFB TR/7 and by the CCT at LSU.

References

- [1] Pretorius F 2005 *Phys. Rev. Lett.* **95** 121101
- [2] Pretorius F 2006 *Class. Quantum Grav.* **23** S529–S552
- [3] Baker J G, Centrella J, Choi D I, Koppitz M and van Meter J 2006 *Phys. Rev. D* **73** 104002
- [4] Campanelli M, Lousto C O and Zlochower Y 2006 *Phys. Rev. D* **73** 061501(R)
- [5] Baker J G, McWilliams S T, van Meter J R, Centrella J, Choi D I, Kelly B J and Koppitz M 2006 Gr-qc/0612117
- [6] Baker J G, Centrella J, Choi D I, Koppitz M, van Meter J and Miller M C 2006 *Astrophys. J.* **653** L93–L96
- [7] González J A, Sperhake U, Brügmann B, Hannam M and Husa S 2006 Gr-qc/0610154
- [8] Campanelli M, Lousto C O and Zlochower Y 2006 *Phys. Rev. D* **74** 041501
- [9] Campanelli M, Lousto C O and Zlochower Y 2006 *Phys. Rev. D* **74** 084023
- [10] Campanelli M, Lousto C O, Zlochower Y, Krishnan B and Merritt D 2006 Gr-qc/0612076
- [11] Baker J G, Campanelli M, Pretorius F and Zlochower Y 2007 Gr-qc/0701016
- [12] Seidel E and Suen W M 1992 *Phys. Rev. Lett.* **69**(13) 1845–1848
- [13] Alcubierre M and Brügmann B 2001 *Phys. Rev. D* **63** 104006
- [14] Brügmann, Bernd, Tichy, Wolfgang, Jansen and Nina 2004 *Phys. Rev. Lett.* **92** 211101
- [15] Alcubierre M, Brügmann B, Diener P, Guzmán F S, Hawke I, Hawley S, Herrmann F, Koppitz M, Pollney D, Seidel E and Thornburg J 2005 *Phys. Rev. D* **72** 044004
- [16] Diener P, Herrmann F, Pollney D, Schnetter E, Seidel E, Takahashi R, Thornburg J and Ventrella J 2006 *Phys. Rev. Lett.* **96**(12) 121101
- [17] Shoemaker D, Smith K L, Sperhake U, Laguna P, Schnetter E and Fiske D 2003 *Class. Quantum Grav.* **20** 3729–3744 gr-qc/0301111
- [18] Sperhake U, Smith K L, Kelly B, Laguna P and Shoemaker D 2004 *Phys. Rev. D* **69** 024012
- [19] Sperhake U, Kelly B, Laguna P, Smith K L and Schnetter E 2005 *Phys. Rev. D* **71** 124042
- [20] Szilágyi B, Pollney D, Rezzolla L, Thornburg J and Winicour J 2006 Gr-qc/0612150
- [21] Brandt S and Brügmann B 1997 *Phys. Rev. Lett.* **78**(19) 3606–3609
- [22] Alcubierre M, Brügmann B, Diener P, Koppitz M, Pollney D, Seidel E and Takahashi R 2003 *Phys. Rev. D* **67** 084023
- [23] Baker J G, Centrella J, Choi D I, Koppitz M and van Meter J 2006 *Phys. Rev. Lett.* **96** 111102
- [24] Campanelli M, Lousto C O, Marronetti P and Zlochower Y 2006 *Phys. Rev. Lett.* **96** 111101
- [25] Baiotti L and Rezzolla L 2006 *Phys. Rev. Lett.* **97** 141101
- [26] Hannam M, Husa S, Pollney D, Brügmann B and Ó Murchadha N 2006 Gr-qc/0606099
- [27] Nakamura T, Oohara K and Kojima Y 1987 *Prog. Theor. Phys. Suppl.* **90** 1–218
- [28] Baumgarte T W and Shapiro S L 1999 *Phys. Rev. D* **59** 024007
- [29] Alcubierre M, Brügmann B, Dramlitsch T, Font J A, Papadopoulos P, Seidel E, Stergioulas N and Takahashi R 2000 *Phys. Rev. D* **62** 044034
- [30] Alcubierre M, Allen G, Brügmann B, Seidel E and Suen W M 2000 *Phys. Rev. D* **62** 124011
- [31] Alcubierre M, Brügmann B, Diener P, Herrmann F, Pollney D, Seidel E and Takahashi R 2004 Testing excision techniques for dynamical 3D black hole evolutions
- [32] Scheel M A, Pfeiffer H P, Lindblom L, Kidder L E, Rinne O and Teukolsky S A 2006 *Phys. Rev. D* **74** 104006
- [33] Choptuik M W, Goldwirth D S and Piran T 1992 *Class. Quant. Grav.* **9**(3) 721–750
- [34] Ansorg M, Brügmann B and Tichy W 2004 *Phys. Rev. D* **70** 064011
- [35] van Meter J R, Baker J G, Koppitz M and Choi D I 2006 *Phys. Rev. D* **73** 124011
- [36] Thornburg J 1996 *Phys. Rev. D* **54**(8) 4899–4918
- [37] Thornburg J 2004 *Class. Quantum Grav.* **21**(2) 743–766
- [38] Schnetter E, Hawley S H and Hawke I 2004 *Class. Quantum Grav.* **21**(6) 1465–1488
- [39] Savitzky A and Golay M J E 1964 *Analytical Chemistry* **36**(8) 1627–1639
- [40] Karlhede A 1980 *Gen. Rel. Grav.* **12** 693–707